Controlling ghost traps in holographic optical tweezers

Christina Hesseling,[1,2] Mike Woerdemann,[1,*] Andreas Hermerschmidt,[2] and Cornelia Denz[1]

[1]*Institut für Angewandte Physik, Westfälische Wilhelms-Universität Münster, Corrensstrasse 2, 48149 Münster, Germany*

[2]*HOLOEYE Photonics AG, Albert-Einstein-Strasse 14, 12489 Berlin, Germany*

**Corresponding author: woerde@uni-muenster.de*

Received June 27, 2011; revised August 7, 2011; accepted August 12, 2011; posted August 15, 2011 (Doc. ID 149637); published September 14, 2011

Computer-generated holograms displayed by phase-modulating spatial light modulators have become a well-established tool for beam shaping purposes in holographic optical tweezers. Still, the generation of light intensity patterns with high spatial symmetry and simultaneously without interfering ghost traps is a challenge. We have implemented an iterative Fourier transform algorithm that is capable of controlling these ghost traps and demonstrate the benefit of this approach in the experiment. © 2011 Optical Society of America

OCIS codes: 350.4855, 140.7010, 170.4520, 090.1760, 140.3300.

Holographic optical tweezers have become an indispensable tool in various fields of research. Because of their ability to trap within liquid suspensions, optical tweezers are not only applied in atomic physics and solid-state physics, but have also expanded the possibilities of study in live sciences [1]. Computer-generated phase holograms displayed by spatial light modulators (SLMs) allow for an adaptable formation of trapping patterns. Despite the development of various algorithms for the generation of appropriate holograms, ghost traps (i.e., undesired intensity peaks strong enough to trap particles) are still an issue. The problem is particularly acute when highly symmetric trapping patterns are required [2].

Analytical approaches for the generation of holograms utilizing the complex superposition of gratings and lenses [3] and modifications of this algorithm [2] have been discussed because of the small number of necessary operations compared to iterative methods like the Gerchberg Saxton algorithm [4]. It could be demonstrated that this yields satisfying results whenever asymmetric patterns are required [2]. Still, for patterns with high symmetry, iterative algorithms are able to improve the results significantly [2]. Complete absence of ghost traps accompanied by a good uniformity of the desired traps is achieved by the random mask-encoding algorithm [5], which is an extension of the gratings and lenses approach. Unfortunately, the efficiency is reduced so much that only a few traps can be generated [5]. Polin *et al.* [6] suggested a different approach with a modified setup in which the zeroth order of diffraction and corresponding ghost traps are defocused and blocked while a direct search algorithm is used to find appropriate holograms for optical trapping. However, especially when more than eight phase levels are to be applied in order to exploit more degrees of freedom made available by modern SLMs, direct search algorithms are computationally expensive compared to the classical Gerchberg Saxton algorithm [7], which is an example for iterative Fourier transform algorithms (IFTAs).

We have developed an IFTA for the generation of holograms with 256 phase levels specifically tailored to the application in holographic optical tweezers. The algorithm is capable of generating light fields for the trapping of particles in arbitrary lateral positions, including highly symmetrical configurations, while the number and strength of ghost traps is significantly reduced. The relative intensities of generated ghost traps can be limited to a magnitude that is small enough to ensure that no particle is trapped. This is demonstrated in a holographic optical trapping experiment where ghost traps surrounding a highly symmetrical trapping pattern are reduced by activating the ghost trap control such that only the polystyrene particles in the desired traps remain stably trapped while all particles previously trapped by ghosts leave their positions.

In holographic optical tweezers, a diffractive optical element is positioned in the Fourier plane of the sample plane [8]. The Fourier relation between hologram and image domain is utilized in IFTAs. These algorithms alternate between hologram and image domain, applying forward and inverse Fourier transformations (fFTs and iFTs), while in each domain the light field is altered to satisfy the respective constraints. As visualized in Fig. 1, this process is repeated until the exit condition is fulfilled. The illumination by an approximately plane wave imposes the constraint of a spatially constant amplitude in the hologram domain. The image domain constraints are given by the desired amplitude distribution while the phase is completely free. Gerchberg and Saxton suggested replacing the achieved amplitude distribution in the image domain by the desired amplitude distribution to generate the input of the next iteration [4]. In a more sophisticated approach, the amplitudes are altered with feedback that promises a reduced error after the next iteration of the algorithm. Such an adaptive replacement scheme can be written in the form of square matrices with $A^{(k)}$ as the amplitude distribution after iteration k of

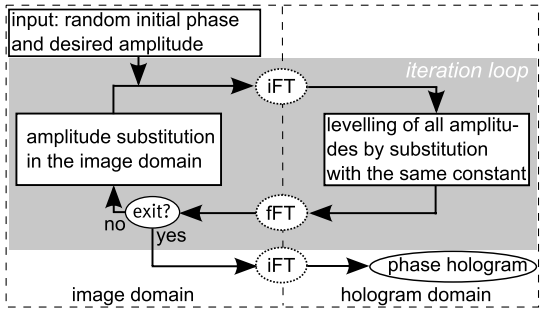

Fig. 1. Iterative Fourier transform algorithm.

the algorithm, $B^{(k+1)}$ as the input amplitude distribution for iteration $k+1$, and A as the desired amplitude distribution [9]

$$B_{(p,q)}^{(k+1)} = A_{(p,q)}^{(k)} + \beta(A_{(p,q)} - A_{(p,q)}^{(k)}) \quad \forall\ (p,q) \in S \qquad (1)$$

with $\beta > 0$ determining the strength of the feedback and S as the set of points in the image domain. The desired amplitude distribution is retrieved from the intensity distribution of the desired traps while no intensity should be diffracted anywhere else.

The simplicity of the desired amplitude distribution for optical trapping is the onset of this paper. The idea is to reduce the number of constraints in the image domain to the number of desired trapping positions and positions where ghost traps tend to appear within an area of interest that is regarded as relevant in the concrete experiment. Furthermore, a threshold value can be defined when an undesired intensity peak in the sample plane becomes a ghost trap. Below this value, the intensity peak is too weak to trap particles and thus no obstacle in the trapping experiment. The increased number of degrees of freedom can be used to ensure that the intensity in the area of interest is controlled.

One challenge is the identification of potential ghost trap positions for arbitrary initial phase distributions. By using the IFTA shown in Fig. 1 with an amplitude substitution in the image domain given by Eq. (1), where S is the set of positions of the desired traps, holograms have been generated for different initial phase distributions and various values of the feedback parameter β in the range from 0 to 3. While no considerable dependence of the ghost trap positions on the feedback parameter β could be observed, the initial phase distribution has strong influence. This can be seen in Fig. 2, which shows the spatial distribution of six desired traps surrounded by all ghost traps that exceed 5% of the mean intensity of the desired traps in the numerical reconstructions of the holograms. These holograms have been generated with the identical iteration loop but for three different initial phase distributions. These examples show that ghost traps do not only depend on the symmetry of the desired traps but also on the initial phase distribution of the algorithm.

For this reason, the amplitude substitution in the IFTA is altered to the structure shown in Fig. 3. When the algorithm returns to the image domain for the first time, all relevant positions in which the relative intensities exceed a threshold of 3% of the maximum intensity of the desired traps are identified. In addition to the feedback applied in the desired trapping positions according to Eq. (1), the amplitudes in the identified ghost trap positions are

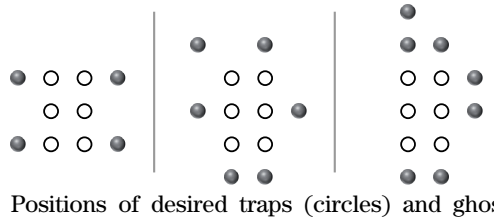

Fig. 2. Positions of desired traps (circles) and ghost traps (gray dots) for three different initial phase distributions in the IFTA without ghost trap control.

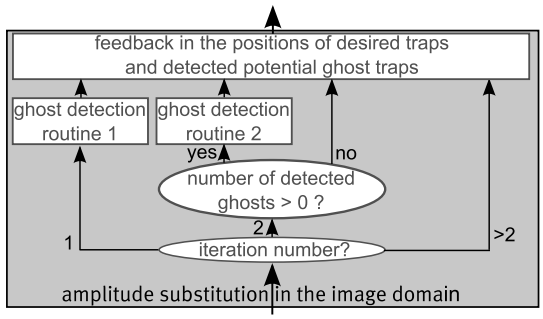

Fig. 3. Flow chart of the modified amplitude substitution in the image domain with ghost trap control.

altered. Because of the existence of a threshold value for ghost traps, the amplitudes in the potential ghost trap positions need not to be substituted by zero. Instead, they are altered with the adaptive feedback with a desired amplitude value of 3% of the mean desired amplitudes in the trapping positions in order to reduce the influence of this modification on the rest of the image. When the algorithm returns to the image domain for the second time, additional intensity peaks tend to appear in positions that are related symmetrically to the array of desired traps and to the previously found potential ghost traps. Thus, additional ghost traps are identified and included in the feedback. In the following iterations, the feedback in the desired traps and in the potential ghost positions is repeated with the respective desired amplitude values until the exit condition is met.

In order to test the results of the algorithm for holographic optical trapping, we employed a holographic optical tweezers setup, as described in [10], containing a high-resolution liquid crystal on silicon phase-only SLM ("PLUTO" from Holoeye Photonics), which allows for the application of 256 phase levels in the holograms. Therefore, errors due to phase quantization effects can be neglected. The intensity values in the sample plane are retrieved from images recorded by a calibrated CCD camera that monitors the sample plane when the sample is replaced by a mirror. A particularly challenging desired pattern with high symmetry, consisting of six traps with homogeneous desired intensity values, is chosen. The algorithm with ghost trap control is exited when the maximum intensity of all detected potential ghost traps does not exceed 5% of the maximum intensity of the desired traps. This is the approximate threshold value when an intensity peak becomes a ghost trap in the used setup. In order to ensure reasonable computational costs, the loop executes ten iterations at maximum. Ten iterations are also used to generate a reference hologram without ghost trap control. The positions are defined in a coordinate system where the origin refers to the position of the zeroth order of diffraction in the reconstruction. In this demonstration, the desired minimum distance between a desired trap position and the nearest ghost trap is defined as 22 pixels, which corresponds to 14 μm in the sample plane.

Figure 4 shows the intensities of traps in the numerical and experimental reconstructions of the generated holograms. Intensity values are given relative to the mean intensity of the desired traps. It can be seen that, within the area of interest, from previously ten undesired intensity

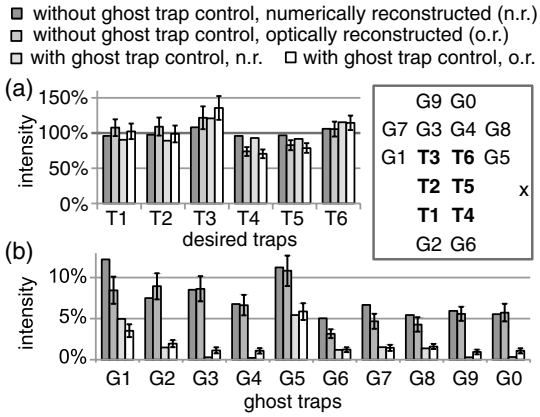

Fig. 4. Intensities relative to the mean intensity of the desired traps in the numerical and optical reconstructions of holograms generated with and without ghost trap control. Positions of desired traps ($T1, \ldots T6$) and ghost traps ($G1, \ldots G0$) exceeding a value of 5% in the optical or numerical reconstruction are indicated in the inset. Nearest neighbor traps have a distance of 10 pixels at the numerical grid and only ghost traps in the area of interest (see text) are shown. The intensity of the zeroth order of diffraction (marked with x) is not shown.

peaks exceeding 5% of the mean intensity in the desired trapping positions, just a single one remains with an intensity value of 5.4% in relation to the mean intensity of the desired traps (i.e., with 4.5% of the maximum intensity value). The only ghost traps that are strengthened when the ghost trap control is applied are in positions that have not been included in the feedback as they are outside the area of interest. With and without ghost trap suppression, a diffraction efficiency of approximately 80% is achieved while all intensity peaks are perfectly capable of trapping particles. This is demonstrated by replacing the mirror in the sample plane by a sample of polystyrene particles with a diameter of 2.27 μm suspended in water. The recorded camera images are shown in Fig. 5. In Fig. 5(a), a hologram generated without ghost trap control is applied. Though a pattern of six traps is desired, ten particles are stably trapped, i.e., the particles can be moved within the medium without escaping the traps. As soon as the ghost trap control is applied, the particles within previous ghost trap positions start to leave these positions due to their Brownian motion. Thus, 10 s after the ghost trap control has been switched on, there can be no doubt that they move freely in the fluid.

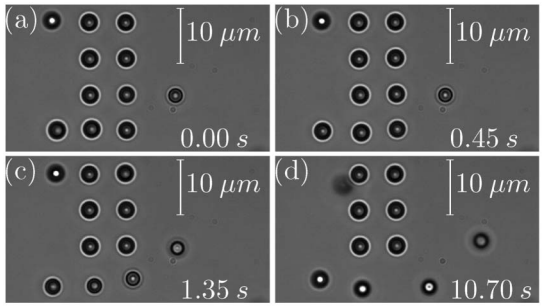

Fig. 5. (a) Ten particles are stably trapped in six desired and four undesired traps on a symmetrical grid. (b)–(d) By applying the ghost trap control, the particles trapped by ghosts drift away (Media 1).

In summary, the geometry and the input phase distribution decide upon the positions and the relative strengths of generated ghost traps. The implemented and demonstrated IFTA minimizes the number of constraints in the image domain by selectively identifying and suppressing potential ghost traps. This algorithm is tailored to optical trapping applications and generates optimized holograms for arbitrary patterns within the physically realizable limits. While the desired traps remain and the diffraction efficiency is approximately constant, ghost traps are significantly reduced below a threshold value that prohibits particle trapping.

References

1. M. Padgett, J. Molloy, and D. McGloin, eds., *Optical Tweezers: Methods and Applications*, Series in Optics and Optoelectronics (Taylor and Francis, 2010).
2. J. Curtis, C. Schmitz, and J. Spatz, Opt. Lett. **30**, 2086 (2005).
3. J. Liesener, M. Reicherter, T. Haist, and H. J. Tiziani, Opt. Commun. **185**, 77 (2000).
4. R. Gerchberg and W. Saxton, Optik **35**, 237 (1972).
5. M. Montes-Usategui, E. Pleguezuelos, J. Andilla, and E. Martin-Badosa, Opt. Express **14**, 2101 (2006).
6. M. Polin, K. Ladavac, S.-H. Lee, Y. Roichman, and D. G. Grier, Opt. Express **13**, 5831 (2005).
7. R. Di Leonardo, F. Ianni, and G. Ruocco, Opt. Express **15**, 1913 (2007).
8. S. Zwick, T. Haist, M. Warber, and W. Osten, Appl. Opt. **49**, F47 (2010).
9. E. Dufresne, G. Spalding, M. Dearing, S. Sheets, and D. Grier, Rev. Sci. Instrum. **72**, 1810 (2001).
10. M. Woerdemann, S. Gläsener, F. Hörner, A. Devaux, L. De Cola, and C. Denz, Adv. Mater. **22**, 4176 (2010).